Journal of Alloys and Compounds 323–324 (2001) 351–354
www.elsevier.com/locate/jallcom

Pulsed, broadly tuneable, photoacoustic study of rare-earth doped $LiNbO_3$

E. Cantelar[a], R.E. Di Paolo[a,b], J.O. Tocho[b], F. Cussó[a,*]

[a]*Departamento de Física de Materiales, C-IV, Universidad Autónoma de Madrid, 28049 Madrid, Spain*
[b]*Centro de Investigaciones Ópticas (CIOp), Casilla de Correo 124, 1900 La Plata, Argentina*

Abstract

Rare-earth (RE) doped solids are widely used as optical emitters from the near infrared to the ultraviolet range. A key measurement for such applications, the luminescent quantum efficiency, quantifies the comparison between radiative and non-radiative probabilities, which can be evaluated from luminescence and photoacoustic measurements, respectively. The photoacoustic and luminescence excitation signals can be obtained either under pulsed dual-wavelength excitation or CW tuneable excitation, by using Nd-YAG and Ti:Sapphire lasers. In the present work, we demonstrate the use of pulsed, broadly tuneable, excitation using an optical parametric oscillator (OPO), extending the spectral range of application covering practically all the near infrared to the ultraviolet range, and accessing any RE emitting level. The procedure is applied to RE-doped lithium niobate ($LiNbO_3$), a material of great interest for optoelectronic applications.

Keywords: Trivalent rare-earth; Lithium niobate; Photoacoustic; Luminescence

---

1. Introduction

The luminescence quantum efficiency is one of the most relevant characteristics of the optical properties of rare-earth activated luminescence solids. In spite of this, this quantity has been usually determined by indirect measurements, by the comparison of the experimental lifetimes and the calculated radiative values.

A fully experimental determination of this magnitude is possible using luminescence and photoacoustic techniques. The photoacustic methods, which were first applied to gas and liquid samples [1,2], were later extended with some modifications to crystalline materials [3–9]. These methods were dedicated mainly to studying the non-radiative de-excitation channels of different samples. However, the luminescence techniques also have been employed to study the radiative channels. When both luminescence and photoacoustic techniques are simultaneously used to obtain information about luminescent materials, it is possible to determine an absolute value of luminescence quantum efficiency. As an example of this, the simultaneous and multiwavelength measurements of photoacoustic (PAS) and luminescence (LUMS) signals after pulsed laser excitation allow determination of the high quantum efficiency for Eu^{+2} ions in different alkali halides [10,11]. More recently, the use of CW excitation using tunable sources, such as Ti:Sapphire laser, has allowed extension of the method to trivalent rare-earth doped crystals [12].

2. Experimental procedure

The $LiNbO_3$:RE^{3+} codoped crystals used in this work were grown by the Czochralski method with automatic diameter control by crucible weighting system [13]. Dopant concentrations were ~1×10^{20} atoms/cm^3, as determined by total X-ray fluorescence spectrometry.

Pulsed excitation at different wavelengths is achieved by using a Nd:YAG laser, linked to a harmonics generator. A Ti:Sapphire laser pumped with an argon ion laser can be used as CW infrared excitation source over a wide spectral range. The excitation beam can be modulated at frequency by using a mechanical chopper. Another pulsed excitation source, broadly tuneable, is the master optical parametric oscillator (MOPO). With this source the spectral range of excitation is extended from the near infrared to the ultraviolet. Fig. 1 shows the spectral range and the tuning possibilities of the three excitation sources mentioned in

---

[*]Corresponding author. Tel.: +34-91-397-4765; fax: +34-91-397-8579.

E-mail address: fernando.cusso@uam.es (F. Cussó).

0925-8388/01/$ – see front matter
PII: S0925-8388(01)01034-9

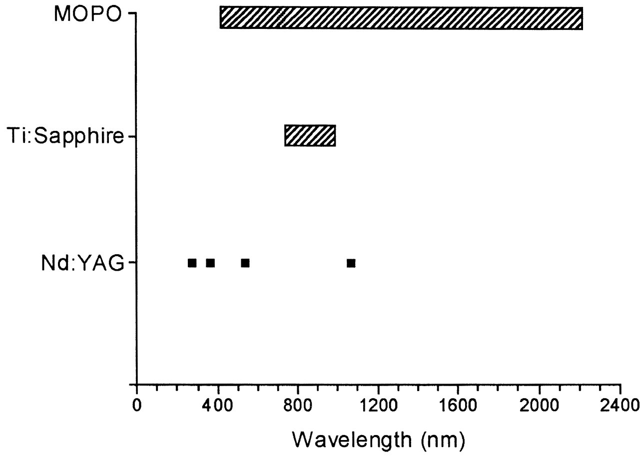

Fig. 1. Spectral range and tuning possibilities of the three excitation sources mentioned in this work (Nd:YAG, Ti:Sapphire and master optical parametric oscillator (MOPO)).

this work. The use of the MOPO is advisable as it could allow access to practically any RE multiplet.

The luminescence and photoacoustic excitation spectra were measured synchronously. Both signals were averaged and recorded using an EG&G lock-in amplifier model 7220 DSP. The luminescence signal was analyzed through an ARC monochromator model SpectraPro 500-i and then detected by an InGaAs and a Si photodiode, for the infrared and visible radiation, respectively. The photoacoustic signal was detected by using a resonant piezoelectric transducer [14].

3. Results and discussion

Fig. 2 illustrates the use of dual-wavelength simultaneous measurements of PAS and LUMS, using pulsed laser excitation, applied to the green emission of Er^{3+} ions in lithium niobate [15]. The optical absorption spectrum of Er^{3+} ions in $LiNbO_3$ is shown in Fig. 2(a) showing the different absorption bands from the fundamental $^4I_{15/2}$ level to the different excited states.

Er^{3+} ions can be excited with the second ($2\omega_0$) and third ($3\omega_0$) harmonics of the Nd:YAG laser, leading initially to the $^4S_{3/2}$ and $^2G_{7/2}$ levels, respectively (see arrows in Fig. 2(a)). A non-radiative multiphonon relaxation connects the $^2G_{7/2}$ level with the $^4S_{3/2}$ level, which emits green luminescence associated with the transition $^4S_{3/2}\rightarrow{}^4I_{15/2}$.

After pulsed excitation, using several different pulse energies with the Nd:YAG laser, the green luminescence of the $^4S_{3/2}\rightarrow{}^4I_{15/2}$ transition and the photoacoustic signal are simultaneously measured. Fig. 2(b) shows the linear correlation between PAS and LUMS. This linear behavior depends on the excitation wavelength and the difference in slope between $2\omega_0$ and $3\omega_0$ excitation, and it is a consequence of the non-radiative connection between the excited states of Er^{3+} ions, which can be used as an internal calibration and allows the determination of the luminescence quantum efficiency.

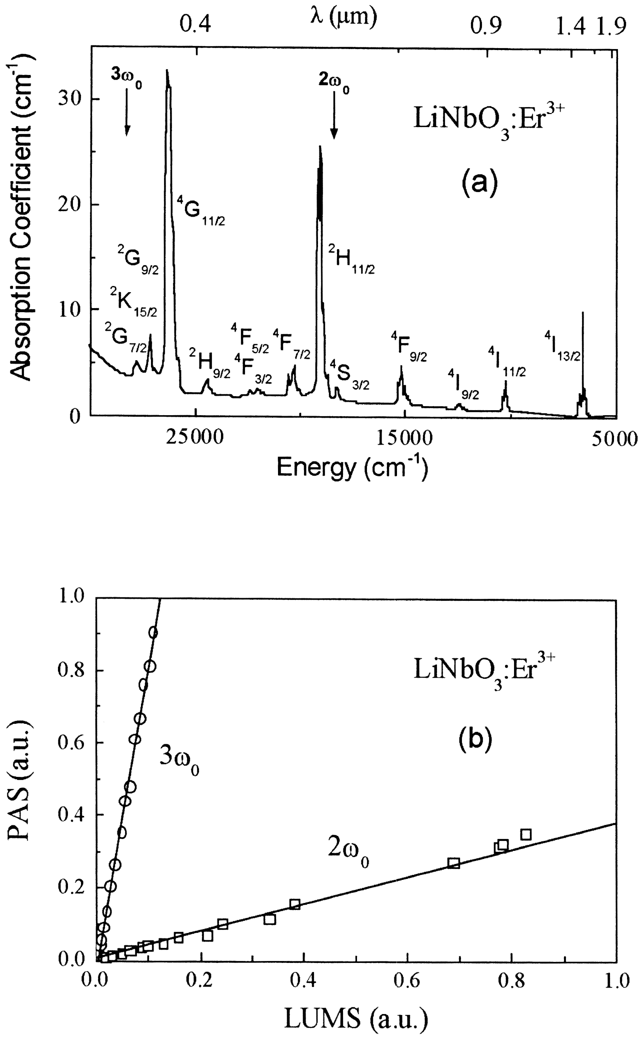

Fig. 2. (a) Absorption spectrum of Er^{3+} ions in $LiNbO_3$, showing (arrows) the pumping used in the photoacoustic and luminescence measurements. (b) Photoacoustic and luminescence signals obtained at two wavelength excitations (355 and 532 nm).

In spite of the advantages of using this method, an inspection of the absorption spectrum in Fig. 2(a) immediately reveals the limitations of using discrete excitation ($2\omega_0$, $3\omega_0$) in the case of Er^{3+}, which impedes access to more adequate (intense) excitation bands. This difficulty can be overcome by using tuneable excitation sources. In particular, for Nd^{3+} ions, the tuneability of the Ti:Sapphire laser allows excitation of the $^4F_{3/2}$ multiplet either directly or to the upper $^4F_{7/2}$ and $^4F_{5/2}$ excited multiplets. Fig. 3(a) shows the results corresponding to the photoacoustic and luminescence excitation spectra. The shape of the absorp-

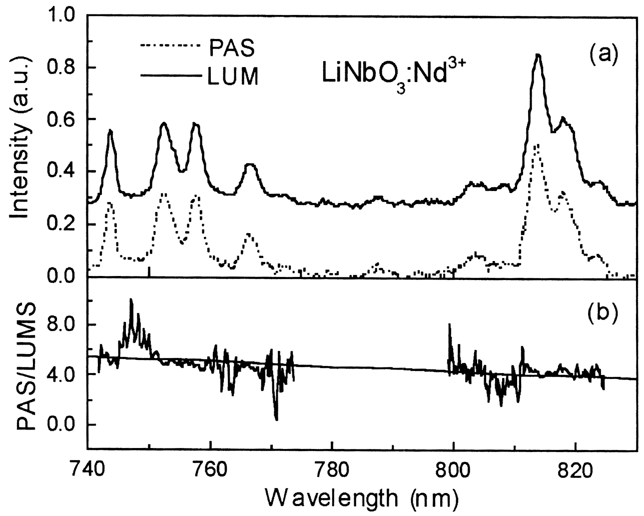

Fig. 3. (a) Photoacoustic and luminescence excitation of the 1.064-μm emission ($^4F_{3/2} \rightarrow {}^4I_{11/2}$) by tuning over the $^4F_{5/2}$–$^4F_{7/2}$ levels of LiNbO$_3$:Nd^{3+}. (b) Comparison of PAS–LUMS. The quotient between both signals is fitted with a straight line.

tion bands is clearly identified in the PAS or LUMS excitation spectra, which obviously provides more information than dual-wavelength excitation.

The quotient between the photoacoustic (PAS) and luminescence (LUMS) signals is shown in Fig. 3(b) and it has been demonstrated [16] that it should be linearly dependent on the excitation wavelength, λ_E,

$$PAS/LUMS = C(1 - \phi\,(\lambda_E/\lambda_F)) \quad (1)$$

where C is an experimental constant, and λ_F and λ_E are the fluorescence and excitation wavelengths, respectively. From the fitting of these data using Eq. (1), a luminescence quantum efficiency $\phi = 0.95$ for the $^4F_{3/2} \rightarrow {}^4I_{11/2}$ transition Nd^{3+} in LiNbO$_3$ is obtained.

Nevertheless, Ti:Sapphire excitation still suffers from limitations. While it has been shown that continuous tuning is possible over the $^4F_{7/2}$ and $^4F_{5/2}$ Nd^{3+} absorption bands, the wavelength tuneability is still limited (Fig. 1). As an example, Fig. 4 shows how in the case of Yb^{3+} ions, Ti:Sapphire excitation only allows coverage of a small fraction of its absorption band. Fig. 4(a) shows the absorption spectrum of LiNbO$_3$:Yb^{3+} and Fig. 4(b) shows the Ti:Sapphire laser emission (dashed line). As a consequence of this, the PAS obtained with such a source appears strongly distorted (see solid line in Fig. 4(b)), and the high wavelength portion of the spectrum is lost.

Therefore, in order to fully exploit the potential of this method (simultaneous PAS and LUMS measurements), broadly tuneable sources are required. Fortunately, a MOPO has recently become available. This source provides pulsed excitation, broadly tuneable, allowing access to any RE emitting level (Fig. 1). The advantage of this source can be observed in Fig. 4(c), where the PAS–LUMS measurements of LiNbO$_3$:Yb^{3+} obtained with a MOPO are shown. Comparing these results with those obtained under Ti:Sapphire excitation, it can be observed that the PAS and LUMS spectra obtained now provide an excellent reproduction of the absorption spectrum.

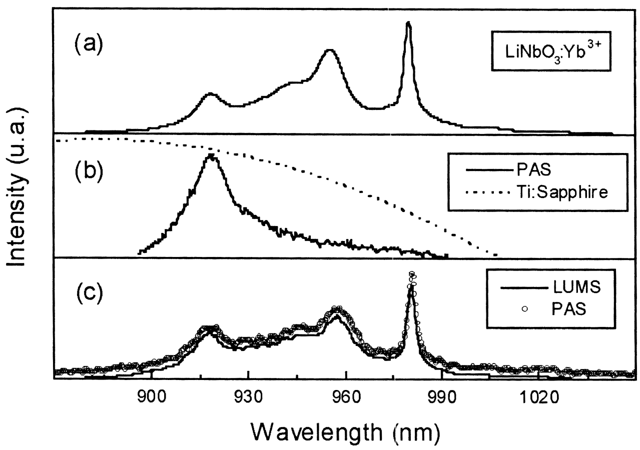

Fig. 4. (a) LiNbO$_3$:Yb^{3+} absorption spectrum. (b) Photoacoustic spectrum obtained by exciting with Ti:Sapphire laser (solid line), and Ti:Sapphire laser emission (dashed line). (c) Photoacoustic and luminescence spectra of LiNbO$_3$:Yb^{3+} obtained by exciting with MOPO (circles and solid line correspond to PAS and LUMS, respectively).

The fact that this source can be tuned over any RE transition, allows the design of experiments in which is possible to access, following in order the low-lying levels, from the ground state to all other levels of the ion. Nevertheless, the extended tuneability range together with some energy-pulse instability affects the signal-to-noise ratio. Recent reports on the use of non-standard lock-in amplifier (LIA) techniques, such as pulse-duration-scanned LIA [17], indicate the possibility of substantial signal-to-noise ratio improvements. The optimum use of the devices associated with the PAS–LUMS detection should reduce the sampling times (at the moment these times are high, tens of minutes for the signals shown in Fig. 4(c)) and improve the electronic data processing.

Finally, in the case of anisotropic crystals (such as LiNbO$_3$) the use of polarised excitation also offers the possibility of accessing transitions exhibiting different polarisation selection rules, as has been already demonstrated in LiNbO$_3$:Yb^{3+} [4].

Acknowledgements

This work was partially supported by DGES Ministerio de Eduación y Cultura (project PB97-0019) and Comunidad de Madrid (07T/0026/1998). One of the authors (R.E. Di Paolo) wishes to thank the Ministerio de Educación y Cultura of Spain for a grant.

References

[1] C.K.N. Patel, A.C. Tam, Rev. Mod. Phys. 53 (1981) 517.
[2] A.C. Tam, Rev. Mod. Phys. 58 (1986) 381.
[3] E. Rodriguez, J.O. Tocho, F. Cussó, Phys. Rev. B 47 (1993) 14049.
[4] J.A. Muñoz, J.O. Tocho, F. Cussó, Appl. Opt. 37 (1998) 7096.
[5] J.C. Murphy, M.C. Aamodt, J. Appl. Phys. 48 (1977) 3502.
[6] L.D. Merkle, R.C. Powell, Chem. Phys. Lett. 46 (1977) 303.
[7] R.S. Quimby, W.N. Yen, Opt. Lett. 3 (1978) 181.
[8] J. Etxebarría, J. Fernández, J. Phys. C Solid State Phys. 16 (1983) 3803.
[9] J.A. Muñoz, J.O. Tocho, F. Cussó, Europhys. Lett. 43 (1998) 159.
[10] J.A. Muñoz, R.E. Di Paolo, J.O. Tocho, F. Cussó, B. Castañeda, R. Pérez-Salas, R. Aceves, M. Barbosa-Flores, J. Phys. Condens. Matter. 10 (1998) 4113.
[11] E. Rodriguez, J.A. Muñoz, J.O. Tocho, F. Cussó, J. Phys. Condens. Matter. 6 (1994) 10625.
[12] J.A. Muñoz, J.O. Tocho, F. Cussó, in: F. Scudieri, M. Bertolotti (Eds.), Photoacoustic and Photothermal Phenomena: 10th International Conference, AIP Conference Proceedings 463, American Institute of Physics, Woodbury, New York, 1999, p. 256.
[13] S. Braslavsky, S.E. Heihoffk, in: J.C. Scaiano (Ed.), Handbook of Organic Photochemistry, Vol. 1, Chemical Rubber Company, Boca Raton, FL, 1989, p. 327, Chapter 14.
[14] E. Cantelar, J.A. Muñoz, J.A. Sanz-García, F. Cussó, J. Phys. Condens. Matter. 10 (1998) 8893.
[15] J.A. Muñoz, R.E. Di Paolo, R. Duchowicz, J.O. Tocho, F. Cussó, Solid State Commun. 107 (1998) 487.
[16] F. Cussó, J.A. Muñoz, E. Cantelar, J.O. Tocho, E. Rodrigo, J. Lumin. 87–89 (2000) 620.
[17] A. Mandelis, S. Paoloni, L. Nicolaides, Rev. Sci. Instrum. 71 (2000) 2240.